Journal of Neuroradiology 46 (2019) 248–255

Available online at ScienceDirect www.sciencedirect.com

Elsevier Masson France EM|consulte www.em-consulte.com

Original Article

# Post-mortem X-ray computed tomography (PMCT) identification using ante-mortem CT-scan of the sphenoid sinus

Lucile Deloire [a], Idris Diallo [b], Romain Cadieu [a], Mathieu Auffret [c], Zarrin Alavi [d], Julien Ognard [a], Douraïed Ben Salem [a,e,*]

[a] Forensic Imaging Unit, University Hospital of Brest, boulevard Tanguy-Prigent, 29609 Brest cedex, France
[b] Imaging and Radiology Department, Cornouaille Hospital of Quimper, 14 bis, avenue Yves-Thépot, 29107 Quimper cedex, France
[c] Imaging and Radiology Department, Brittany Atlantic Hospital of Vannes, 20, boulevard Général-Maurice-Guillaudot, 56000 Vannes, France
[d] Inserm CIC 1412, University Hospital of Brest, boulevard Tanguy-Prigent, 29609 Brest cedex, France
[e] LaTIM, Inserm UMR 1101, Université de Bretagne Occidentale, 2, avenue Foch, 29609 Brest cedex, France

ARTICLE INFO

*Article history:*
Available online 1 September 2018

*Keywords:*
Sphenoid sinus
Forensic identification
Post-mortem computed tomography

ABSTRACT

*Purpose.* – To evaluate forensic identification of individuals through visual comparison of sphenoid sinus anatomical configuration using ante- and post-mortem CT-scans.
*Method and materials.* – Ante- and post-mortem head CT-scan of 33 individuals were retrospectively collected. Ten head CT-scans were randomly selected from various neurological contexts and added to the ante-mortem group. Ten other head CT-scans were randomly selected from our post-mortem PACS and added to the post-mortem group. These CT-scans were assigned into 2 groups for analysis: an ante-mortem group (33 + 10) and a post-mortem group (33 + 10). For ethics and to avoid identification bias, CT-scans were anonymized – not showing any head structure but only sphenoid sinuses. An anatomical based classification system using the sphenoid sinuses anatomical variations was created according to anatomical and surgical literature. This classification was used by readers to identify in two different steps a maximum of matched and then unmatched scans.
*Results.* – The first reader had a sensitivity of 100% [CI: 89.4%–100%] and a specificity of 100% [CI: 99.8%–100%]. Sensitivity and specificity were respectively 93.9% [CI: 79.8%–99.3%] and 99.9% [CI: 99.6%–100%] for the second reader. Positive and negative predictive values were respectively 100% [CI: 89.4%–100%] and 100% [CI: 99.8%–100%] for the first reader. Positive and negative values were respectively 96.9% [CI: 83.8%–99.9%] and 99.9% [CI: 99.7%–100%] for the second reader. Inter-reader variability was estimated by Cohen's kappa and an excellent agreement was found.
*Conclusion.* – We reported an excellent validity and reliability of subjective visual comparison of ante- and post-mortem CT-data using an anatomical based classification of the sphenoid sinus.


## Introduction

Forensic identification is the mainstay of the workflow in forensic investigation. Radiological techniques may be used when the conventional methods (DNA samples, fingerprints, teeth records) [1] are not available. But this identification using radiographic techniques can be only performed if ante-mortem images are available. Post-mortem computed tomography (PMCT) could determine victims' identity, presence of hazardous materials, and gather evidence to determine the cause of death [2]. That is made possible by reformatting and volume rendering, associated with high spatial resolution [3]. Furthermore, low cost and low time consuming process are additional advantages of the PMCT [4]. Also, the conservation of images and their reconstructions [3], transmission and use in forensic telemedicine are major assets [3]. Difficulties of identification in mass fatality incident depend mainly on the context and number of victims. It also depends on the importance of the fragmentation and on the decomposition of bodies as well as the availability of the scanner [5]. A mobile post-mortem CT-scanner was primarily used in 2004 [6] and applied for the first time to a mass fatality incident (car accident) in 2006 [7].

Many forensic identification radiological technics have been described: dental records [8–11], patella [12,13], mandibular lingual canals [14], frontal sinus [15–18], discrete traits [19]. All these structures can be altered or destroyed if severe damages occur

* Corresponding author at: Imagerie Médico-Légale, hôpital de la Cavale Blanche, CHRU Brest, 29609 Brest cedex, France.
*E-mail address:* douraied.bensalem@chu-brest.fr (D. Ben Salem).

https://doi.org/10.1016/j.neurad.2018.08.003
0150-9861/

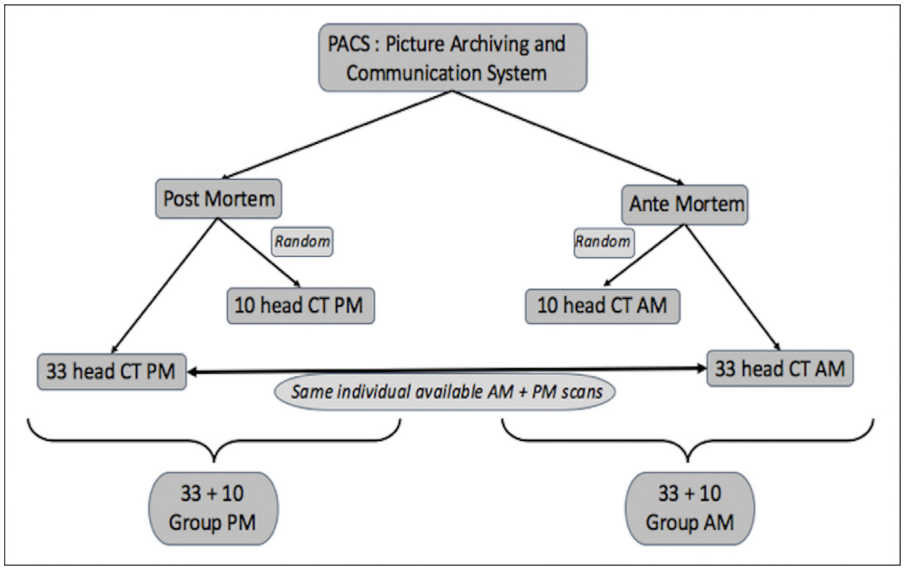


**Fig. 1.** Flowchart of study. AM: ante-mortem; PM: post-mortem.

depending on their localization, limiting their contribution in the identification process. Sphenoid sinuses are located in the center of the skull base [20], being relatively protected of severe damage. Their anatomy, pneumatization (degrees and directions) is extremely variable between individuals [21,22]. For those reason, they can play an essential role in forensic identification.

One study focused on the contribution of the CT of the anatomical aspects of the sphenoid sinuses to individual identification [23]. However, this study has been carried out on living individuals.

The aim of our study was to evaluate forensic identification of individuals through visual comparison of sphenoid sinus anatomical configuration using ante- and post-mortem CT-scans.

## Method and materials

This monocentric retrospective study was conducted in a university hospital between January 2009 and December 2015. Ante-mortem CT-scan used for this study were the same as in a previous one [23]. PMCT conduct was authorized by the French authorities' general attorney.

### *Population*

The study was based on 53 cases:

- 33 individuals who had both ante- and post-mortem CT-scans;
- 10 head CT-scan randomly selected from various neurological contexts;
- 10 head CT-scan randomly selected from the post-mortem PACS.

The supervisor of the study constituted two groups for analysis: the ante-mortem group (AM group), constituted of the ante-mortem CT-scans taken from the 33 individuals to which were added the 10 ante-mortem CT-scans and the post-mortem group (PM group) constituted of the post-mortem CT-scans taken from the same 33 individuals to which were added the 10 post-mortem CT-scans.

Consequently, there were 43 individuals in the AM group (30 male, 13 female, average age: 53 years old, range 22–78) and in the PM group (31 male, 12 female, average age: 51 years old, range 22–78) (Fig. 1).

The supervisor of this study did not participate to the identification process. All the CT were fully anonymized (Anonymize Function, Advantage Windows 4.1 General Electrics Healthcare, Barrington, USA). Each CT-scan was given a random number using the program "the Hat" (Harmony Hollow Software, 3.1.1.6, Covington, Louisiana, 70435, USA). A number between 1 and 43 was assigned to each CT-scan in 2 work-lists. Two work-lists were created (Advantage Windows 4.1 General Electrics Healthcare, Barrington, USA): an ante-mortem work-list and a post-mortem work-list.

### *Exclusion criteria*

There were no exclusion criteria in this study. All ante- and post-mortem CT-scans saved into our PACS were eligible for inclusion.

### *CT protocol*

A multi-detector CT-scanner [Somatom Definition AS+ ($64 \times 2$ channels), Siemens Healthcare, Forchheim, Germany] was used for AM group. PM CT-scans were performed using a dedicated scan (Mx 8000 IDT, 16 channel, Philips Medical Systems, Best, The Netherlands). Acquisition parameters were: 120 kV, 280 mAs, using a care-dose, 0.6 mm collimation, 1.5 mm for the slice thickness, 0.7 mm pitch, increment of 1 mm, using soft tissue kernels (J 30) for AMCT group. For PMCT group, we used 140 kV, 300 mAs, 1.5 mm collimation, 2 mm for the slice thickness, 0.68 mm pitch, increment of 1 mm, using soft tissue kernels (H 20).

### *Reconstruction*

To prevent surrounding structures (teeth, other sinus, mastoid air cells) from influencing the identification process, a cubic exclusion volume of interest (VOI) was produced by the supervisor on every head CT-scan, in order to extract the sphenoid sinus from the whole acquisition, keeping always less than one centimeter around the sphenoid sinus (Fig. 2). The average VOI size was calculated.

Isometric 1 mm reconstructions were made in 3 planes. Reconstructions of axial slices were performed from ethmoidal roof to brain stem axis, for coronal slices, horizontal line between clinoid process and sagittal slices midline. Reconstructions were made with a soft tissue kernel (J 30 or H 20).

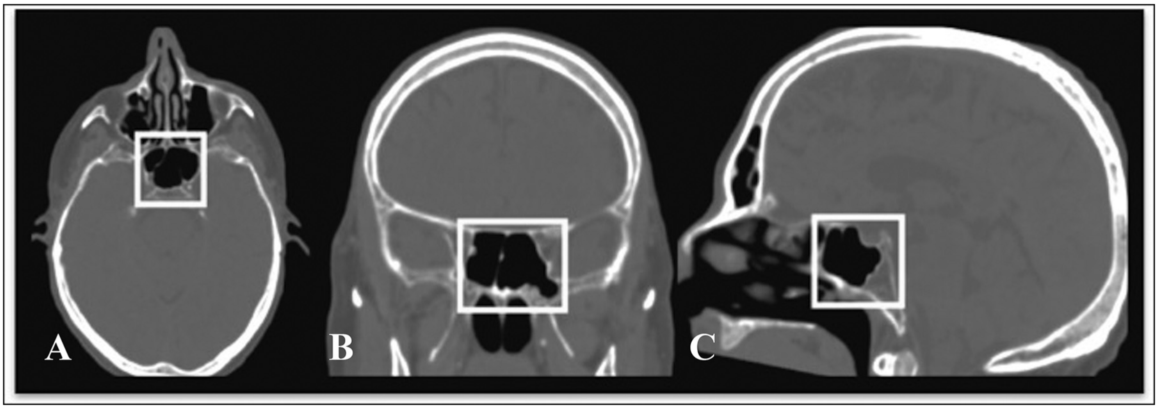


**Fig. 2.** Cubic exclusion volume of interest made in 3 planes, in axial (a), coronal (b) and sagittal (c) slices.

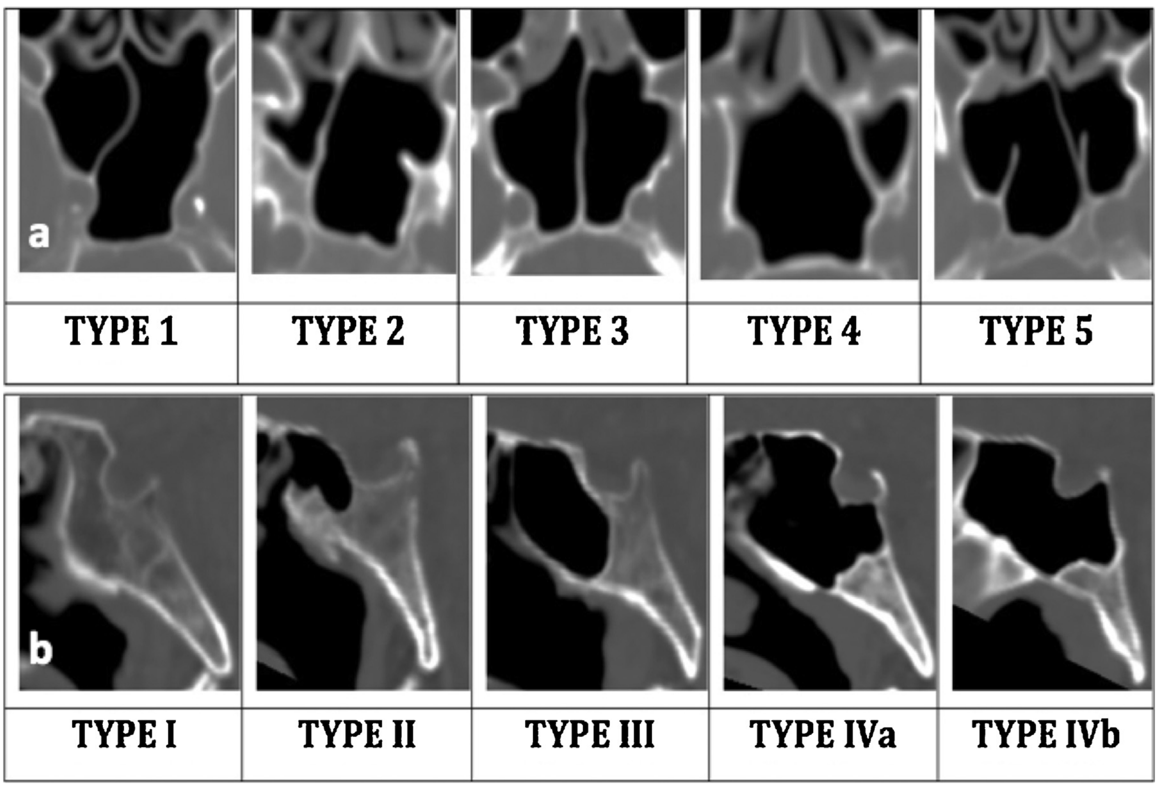


**Fig. 3.** Classification of septum position in axial slices (a) and classification of position of the posterior wall of the sphenoid sinus relative to the sella turcica in sagittal slices (b).

**Table 1**
Table of results of matched answer.

| | Reader No. 1 | | Reader No. 2 | | Cohen's Kappa |
|---|---|---|---|---|---|
| | AM | PM | AM | PM | |
| Matched group right answer | 33 | 33 | 31 | 31 | 0.95 [CI: 90%–100%] |
| Matched group wrong answer | 0 | 0 | 1 | 1 | |

*Identification classification*

In line with in the literature [23], an anatomical classification system of the sphenoid sinus was used and identification process was done according to two primary criteria: septum position in axial slices and position of the posterior wall of the sphenoid sinus in respective to the sella turcica (Fig. 3).

Septum position was taken into account in axial slices as follows:

- type 1: septum was inserted directly on the bony canal of the right carotid artery;
- type 2: septum was inserted at the right side of the median line but not as in type 1;
- type 3: septum was inserted on the median line;
- type 4: septum was inserted at the left side of the median line but not as in type 5;

**Table 2**
Table of results of unmatched answer.

| | Reader No. 1 | | Reader No. 2 | | Cohen's Kappa |
|---|---|---|---|---|---|
| | AM | PM | AM | PM | |
| Unmatched group right answer | 10 | 10 | 9 | 9 | 0.81 [CI: 60.6%–100%] |
| Unmatched group wrong answer | 0 | 0 | 2 | 2 | |

- type 5: septum was inserted directly on the bony canal of the left carotid artery.

Position of the posterior wall of the sphenoid sinus was evaluated in sagittal slices as follows:

- type I conchal: missing or minimal sphenoid sinus;
- type II pre-sellar: posterior wall of the sphenoid sinus was in front of the anterior wall of the sella turcica;
- type III sellar: posterior wall of sphenoid sinus was between anterior and posterior wall of the sella turcica;
- type IV post-sellar: posterior wall of sphenoid was behind the posterior wall of sella turcica.
  Two subgroups were used for type IV:
- type IV a: no air behind sella turcica;
- type IV b: air behind sella turcica.

Readers did not use secondary criteria (infero-lateral, supero-lateral and anterior pneumatization) to facilitate their work [23]. However, presence of accessory septa, carotid siphon calcifications, pterygoid and clinoid process pneumatization could be used if necessary.

*Identification method*

Two readers (reader No. 1: a radiologist with 3 years of experience and reader No. 2: a radiologist with 5 years of experience) participated in the identification process. The first group was used to establish potential identities while the second group, containing the 43 anonymous PMCT, was used to simulate a mass disaster. Each blinded reader was given both ante- and post-mortem work-list and was asked to define the anatomical aspect of sphenoid sinuses to identify the potential victims.

Exact number of matching CT was not known by the two readers. An antatomical classification was used to ease the sinus identification process (Fig. 3). Readers classified every CT-scan of the two work-lists according to the two primary criteria in axial slices (septum position) and sagittal slices (posterior pneumatization). They used multiplanar reformatting (MPR) and bone-weighted density window. After classification of each scan, a visual analysis was carried out for each class of scan. The readings of CT images were done in the 3 planes of space [axial (transverse), sagittal and coronal]. Each reader made a list of matched and unmatched scans to be analyzed by the supervisor.

Reader No. 1 repeated the identification process several months after the first reading.

*Statistical analysis*

Data were analyzed with Statistics Data Analysis (STATA) 13.0, (StataCorp LP, Lakeway Drive, Texas, 77845, USA). Then sensitivity, specificity, positive and negative predictive values were calculated for the answers of each reader. Inter reader agreement was calculated using the Cohen's Kappa, between the answers of the 2 readers and intra reader agreement was calculated between the answers of the reader No. 1. Ninety-five percent confidence intervals (95% CI) for Kappa were calculated using an analytical method.

**Table 3**
Classification of the primary criteria determined by reader No. 2 for every scan.

| List | Axial | Sagittal |
|---|---|---|
| 1 | 5 | IV a |
| 2 | 3 | II |
| 3 | 1 | IV a |
| 4 | 2 | IV b |
| 5 | 1 | IV b |
| 6 | 3 | IV b |
| 7 | 2 | IV a |
| 8 | 3 | II |
| 9 | 2 | IV a |
| 10 | 3 | IV a |
| 11 | 4 | IV a |
| 12 | 1 | III |
| 13 | 4 | IV b |
| 14 | 5 | IV b |
| 15 | 3 | IV b |
| 16 | 5 | IV b |
| 17 | 4 | II |
| 18 | 3 | IV a |
| 19 | 1 | IV b |
| 20 | 3 | III |
| 21 | No septum | III |
| 22 | 2 | IV a |
| 23 | 3 | II |
| 24 | 5 | III |
| 25 | 5 | IV b |
| 26 | 3 | III |
| 27 | 4 | IV b |
| 28 | 4 | II |
| 29 | 3 | IV b |
| 30 | 1 | IV a |
| 31 | 4 | IV b |
| 32 | 2 | IV b |
| 33 | 1 | IV b |
| 1-AM | 1 | IV b |
| 2-AM | 3 | III |
| 3-AM | 4 | III |
| 4-AM | 2 | IV b |
| 5-AM | 2 | IV b |
| 6-AM | 1 | IV b |
| 7-AM | 2 | IV b |
| 8-AM | 3 | IV b |
| 9-AM | 4 | IV b |
| 10-AM | 2 | IV b |
| 1-PM | 2 | III |
| 2-PM | 5 | IV b |
| 3-PM | 2 | IV a |
| 4-PM | 4 | IV b |
| 5-PM | 5 | I |
| 6-PM | 2 | IV a |
| 7-PM | 1 | IV a |
| 8-PM | 2 | IV a |
| 9-PM | 4 | IV a |
| 10-PM | 2 | IV b |

## Results

Given all 43 AM and 43 PM CT-scans sorted, readers chose between 1849 combinations.

Reader No. 1 correctly identified 33 pairs of CT and the 10 unmatched CT during his two readings. Whereas reader No. 2 correctly identified 31 pairs of CT and 9 unmatched CT. He wrongly identified a pair (AM + PM) of CT when trying to match 2 CT. He wrongly unmatched 2 pairs of CT in the unmatched group

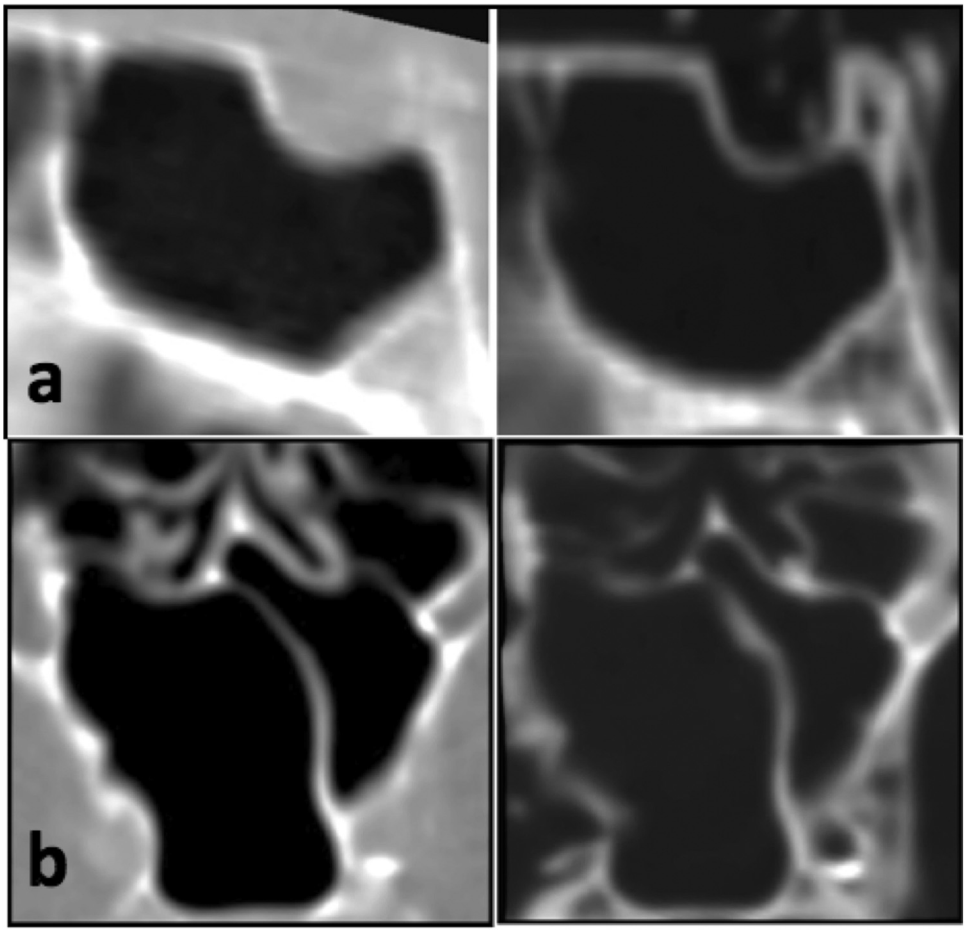


**Fig. 4.** Example of ante-mortem (left) and post-mortem (right) computed tomography (CT)-scan of the same individual in sagittal (a) and axial slices (b).

**Table 4**
Distribution of individuals according to the primary criteria – one individual did not have a septum and was not listed.

| Axial | Sagittal | % |
|---|---|---|
| 1 | III | 1.92 |
| 1 | IV a | 5.77 |
| 1 | IV b | 9.62 |
| 2 | III | 1.92 |
| 2 | IV a | 11.54 |
| 2 | IV b | 13.46 |
| 3 | II | 5.77 |
| 3 | III | 5.77 |
| 3 | IV a | 3.85 |
| 3 | IV b | 7.69 |
| 4 | II | 3.85 |
| 4 | III | 1.92 |
| 4 | IV a | 3.85 |
| 4 | IV b | 9.62 |
| 5 | I | 1.92 |
| 5 | III | 1.92 |
| 5 | IV a | 1.92 |
| 5 | IV b | 7.69 |

(Tables 1 and 2). Intra-reader agreement of the reader No. 1 was 1 [CI: 1.000%–1.000%].

Individual results of the reader No. 2 are presented in Table 3. Distribution of individuals according to the primary criteria was represented in Table 4. One individual did not have a septum and was not listed in this table. In our study, the distribution of sphenoid sinuses in the sagittal slices were: type I in 1.9%, type II in 9.4%, type III in 15.1% and type IV in 26.4% and 47.2% respectively for IV a and IV b. The distribution of sphenoid sinuses in the axial slices were: type 1 in 17.3%, type 2 in 26.9%, type 3 in 23.1%, type 4 in 19.2% and type 5 in 13.5%.

**Table 5**
Table of results of sensitivity, specificity, positive and negative value.

| | Reader No. 1 | Reader No. 2 |
|---|---|---|
| Sensitivity | 100% [CI: 89.4%–100%] | 93.9% [CI: 79.8%–99.3%] |
| Specificity | 100% [CI: 99.8%–100%] | 99.9% [CI: 99.6%–100%] |
| Positive predictive value | 100% [CI: 89.4%–100%] | 96.9% [CI: 83.8%–99.9%] |
| Negative predictive value | 100% [CI: 99.8%–100%] | 99.9% [CI: 99.7%–100%] |

Sensitivity and specificity were both 100% respectively [confidence interval (CI): 89.4%–100%] and [CI: 99.8%–100%] for reader No. 1. Sensitivity and specificity were respectively 93.9% [CI: 79.8%–99.3%] and 99.9% [CI: 99.6%–100%] for reader No. 2 (Table 5).

Positive and negative predictive values were both 100% respectively [CI: 89.4%–100%] and [CI: 99.8%–100%] for reader No. 1. Positive and negative values were respectively 96.9% [CI: 83.8%–99.9%] and 99.9% [CI: 99.7%–100%] for reader No. 2 (Table 5).

Identification process took between 4 and 6 hours for reader No. 1 and No. 2, respectively and 3 hours for the second reading of the reder No. 1 (Fig. 4).

The average VOI size was calculated to 110.09 $cm^3$ [CI: 99.71 $cm^3$–120.47 $cm^3$], it was variable depending on the sinus morphology.

## Discussion

Inter-reader reliability in matching (identification) of sphenoid sinuses was excellent. Readers were blinded to the exact number

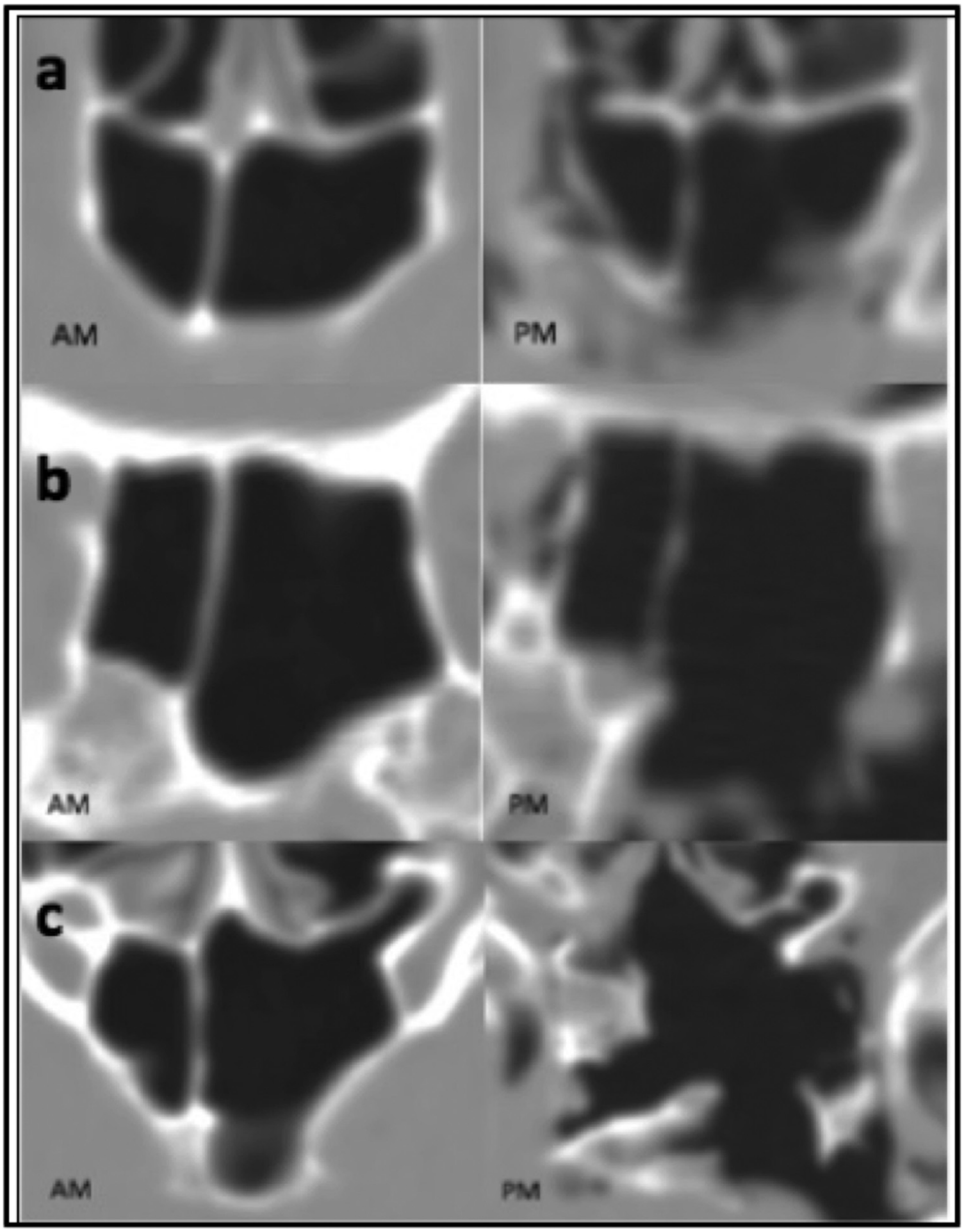


**Fig. 5.** Ante-mortem (AM) and post-mortem (PM) computed tomography (CT)-scan in axial (a and c) and coronal (b) slices, of the same individual. These images show significant traumatic destruction of the sphenoid sinus in PMCT.

of matching CT in the two work-lists. No false identification was made by reader No. 1 (junior expert) and few errors were made by reader No. 2 despite his senior level of forensic experience. Therefore, easiness and reliability are the main strength of this method.

Forensic identification via a radiographic analysis of frontal sinus is a validated technique [24], however sinus X-ray exams are less performed nowadays compared with CT-scans. The CT-scanner has a very good spatial resolution with the possibility of three-dimensional reconstructions [3]. Magnetic resonance imaging is less accessible [25]. In addition, analysis of the paranasal sinuses using magnetic resonance is complicated because of magnetic susceptibility artifacts generated between near air and bone interface [26].

Severe displaced fracture of the walls of the sphenoid sinus is a bias in the post-mortem identification. However, it takes an extremely violent trauma to destroy the sphenoid sinuses which are protected by their disposition in the center of the skull base [20]. Amongst the 43 PMCT only one showed a major destruction of the sphenoid sinus (Fig. 5)

Our method is still relevant when frontal sinuses are destroyed or when dental analysis is impossible (destruction, lack of previous data). Very good values of sensitivity and specificity were found. The agreement rate could have been even higher if other sinuses (e.g. frontal or ethmoidal) had been read too.

The ante-mortem analysis is based on head CT-scan. As head CT-scan is routinely performed nowadays in various neurological contexts, the ante-mortem data base of every hospital PACS is increasing. Furthermore, our two radiologists matched the two work-lists (with 1849 possibilities) in less than 6 hours. This can be explained by the rapidity of the method used (visual analysis of the anatomy of the sphenoid sinus). The only cost of this CT-scan identification would be the cost of post-mortem acquisitions or reconstructions.

The use of an anatomical classification can ease the identification method by shortening the analysis time duration. The ante-

**Table 6**
Table of primary criteria comparison with literature data.

| Reference | Number of subjects | Types in sagittal slices (%) | | | | | Types in axial slices (%) | | | | |
|---|---|---|---|---|---|---|---|---|---|---|---|
| | | I | II | III | IV a | IV b | 1 | 2 | 3 | 4 | 5 |
| Our study | 53 | 1.9 | 9.4 | 15.1 | 26.4 | 47.2 | 17.3 | 26.9 | 23.1 | 19.2 | 13.5 |
| Auffret et al. [23] | 50 | 0 | 2 | 42 | 46 | 10 | 16 | 24 | 26 | 20 | 14 |
| Stokovic et al. [29] | 102 | 2 | 23.5 | 41.2 | 33.3 | | | | | | |
| Akgüll et al. [30] | 202 | 1 | 14.9 | 84.1 (type III, IV a and b) | | | 28.2 | | – | 31.7 | |
| Güldner et al. [31] | 580 | 0.3 | 6.6 | 57.2 | 17.9 | 17.9 | | | | | |
| Hamid et al. [32] | 296 | 2 | 21 | 54.7 | 22.3 | | | | | | |

and post-mortem examination can be classified by their anatomic variability to help at sinus identification process. The aim of our study was not to study sinus classification but sinus identification based on this classification in order to facilitate the matching process. In comparison with the literature, we have found similar results as Auffret et al. [23] about septum position in axial slices (Table 6). It is difficult to analyze these results for the other studies, because the first primary criteria was created by Auffret et al. [23]. About the second primary criteria, the results of the different studies were more heterogeneous. However, types I and II were the least represented.

Ante and PMCT were voluntarily rebuilt with native (standard) acquisition by means of soft filter. They were then read through a bone windowing. This was done to test the visual analysis examination in a worst case scenario, i.e. to reduce variability of identification. CT-scan reconstruction using a bone filter can improve spatial resolution and thus identification process. Despite lower spatial resolution for bone analysis, our study showed a very good agreement rate.

*Limitations*

A major limitation to the application of our technical post-mortem identification is the need of a presumed identity. In the absence of the latter, it is impossible to search the PACS for radiological match. In the future, it would be useful to have a national or even global PACS from which we could extract a larger data set in order to find matches between post-mortem and ante-mortem sphenoid sinuses CT-scans. Moreover, computer-assisted research could be developed thanks to the automatization of sinus segmentation.

In post-mortem conditions, several difficulties are encountered. In some cases, the bodies have an advanced state of decay, sphenoid sinuses filling (water, blood and sand) and sphenoid sinuses fractures (traumatic injury). In our study, one individual had important displaced fractures of the sphenoid sinus. In this case, it was difficult to achieve standardized reconstructions as expected. Only reader No. 1 matched correctly this individual. Regarding this sinus, only the first primary criteria could be applied in axial slices: type 1 (Fig. 5). The posterior wall of the sinus was destroyed and the second primary criteria could not be used. The significant destruction of the sphenoid sinus is a limiting factor in the identification process. In this case, it is almost impossible to classify it according to the 2 primary criteria and therefore to apply our sorting method.

We did not include any children. This identification technique is impossible in the early years of life. Sphenoid sinuses appear in the third year, while, frontal sinuses appear in the sixth years of life [27].

There was a bias in the number of views and visualization of the examination and the windowing changes for each reader, which were not controlled. Only the total time of identification was collected.

Of note, this forensic identification method can be ideal for variety of forensic purposes especially in cases of mass disaster. The major pitfall of PMCT forensic identification in such context would be scanner availability. The latter is scarce or absent in developing countries [5,6,28].

## Conclusion

Our study demonstrated that CT visualization of anatomical aspects of sphenoid sinuses can be used for post-mortem identification purposes. PMCT should be used in comparison with ante-mortem CT and in case of a presumed identity.

Given, the inter-reader agreement and the reader's high specificity and sensitivity, PM CT is reliable and can be easily, readily and cost-effectively used by all radiologists.

## Disclosure of interest

The authors declare that they have no competing interest.

## References


[1] INTERPOL. In: Disaster victim identification guide. Lyon, France: International Criminal Police Organisation; 2014.
[2] Morgan B, Alminyah A, Cala A, O'Donnell C, Elliott D, Gorincour G, et al. Use of post-mortem computed tomography in disaster victim identification. Positional statement of the members of the disaster victim identification working group of the international society of forensic radiology and imaging. J Forensic Radiol Imaging 2014;2(3):114–6.
[3] Dedouit F, Savall F, Mokrane FZ, Rousseau H, Crubezy E, Rouge D, et al. Virtual anthropology and forensic identification using multi-detector CT. Br J Radiol 2014;87(1036):20130468.
[4] Hatch GM, Dedouit F, Christensen AM, Thali MJ, Ruder TD. RADid: a pictorial review of radiologic identification using post-mortem CT. J Forensic Radiol Imaging 2014;2(2):52–9.
[5] Brough AL, Morgan B, Rutty GN. Post-mortem computed tomography (PMCT) and disaster victim identification. Radiol Med (Torino) 2015;120(9):866–73.
[6] Hayakawa M, Yamamoto S, Motani H, Yajima D, Sato Y, Iwase H. Does imaging technology overcome problems of conventional post-mortem examination? A trial of computed tomography imaging for post-mortem examination. Int J Legal Med 2006;120(1):24–6.
[7] Rutty GN, Robinson CE, BouHaidar R, Jeffery AJ, Morgan B. The role of mobile computed tomography in mass fatality incidents. J Forensic Sci 2007;52(6):1343–9.
[8] Kirchhoff S, Fischer F, Lindemaier G, Herzog P, Kirchhoff C, Becker C, et al. Is post-mortem CT of the dentition adequate for correct forensic identification? Comparison of dental computed tomography and visual dental record. Int J Legal Med 2008;122(6):471–9.
[9] Ruder TD, Thali YA, Rashid SNA, Mund MT, Thali MJ, Hatch GM, et al. Validation of post-mortem dental CT for disaster victim identification. J Forensic Radiol Imaging 2016;5:25–30.
[10] Brown KA. Dental identification of unknown bodies. Ann Acad Med Singapore 1984;13(1):3–7.
[11] Lorkiewicz-Muszynska D, Labecka M, Zaba C, Kis-Wojciechowska M, Kolowski J, Sobol J. Difficulties in identification of human corpses and skeletal remains on the basis of dental records and examinations. Arch Med Sadowej Kryminol 2009;59(3):218–24.
[12] Niespodziewanski E, Stephan CN, Guyomarc'h P, Fenton TW. Human identification via lateral patella radiographs: a validation study. J Forensic Sci 2016;61(1):134–40.
[13] Silva RF, Franco A, Mendes SD, Picoli FF, de Azevedo Marinho DE. Human identification through the patella – report of two cases. Forensic Sci Int 2014;238:e11–4.
[14] Mowafey B, Van de Casteele E, Youssef JM, Zaher AR, Omar H, Politis C, et al. Can mandibular lingual canals be used as a forensic fingerprint? J Forensic Odontostomatol 2015;33(2):26–35.
[15] Yoshino M, Miyasaka S, Sato H, Seta S. Classification system of frontal sinus patterns by radiography. Its application to identification of unknown skeletal remains. Forensic Sci Int 1987;34(4):289–99.

[16] Zhang HX, Yang CB, Guo L, Deng ZH. Forensic identification by coding of frontal sinus characteristics of CT. Fa Yi Xue Za Zhi 2011;27(1):13–6.
[17] Besana JL, Rogers TL. Personal identification using the frontal sinus. J Forensic Sci 2010;55(3):584–9.
[18] Ruder TD, Kraehenbuehl M, Gotsmy WF, Mathier S, Ebert LC, Thali MJ, et al. Radiologic identification of disaster victims: a simple and reliable method using CT of the paranasal sinuses. Eur J Radiol 2012;81(2):e132–8.
[19] Verna E, Adalian P, Chaumoitre K, Ardagna Y, Leonetti G, Piercecchi-Marti MD. L'intérêt des caractères discrets en identification médicolégale. Rev Med Leg 2013;4(1):8–15.
[20] Casselman JW. The sphenoid bone: anatomy. J Neuroradiol 2003;30(4):201–10.
[21] Wiebracht ND, Zimmer LA. Complex anatomy of the sphenoid sinus: a radiographic study and literature review. J Neurol Surg 2014;75(6):378–82.
[22] Peele JC. Unusual anatomical variations of the sphenoid sinuses. Laryngoscope 1957;67(3):208–37.
[23] Auffret M, Garetier M, Diallo I, Aho S, Ben Salem D. Contribution of the computed tomography of the anatomical aspects of the sphenoid sinuses to forensic identification. J Neuroradiol 2016;43(6):404–14.
[24] Kullman L, Eklund B, Grundin R. Value of the frontal sinus in identification of unknown persons. J Forensic Odontostomatol 1990;8(1):3–10.
[25] Heimer J, Gascho D, Gentile S, Hatch GM, Thali MJ, Ruder TD. Ante-mortem identification by fusion of MR and CT of the paranasal sinuses. Forensic Sci Med Pathol 2017;13(3):375–8.
[26] Weishaupt D, Köchli VD, Marincek B. How does MRI work? An introduction to the physics and function of magnetic resonance imaging. Berlin Heidelberg: Springer-Verlag; 2006. p. XII [170].
[27] Barghouth G, Prior J, Lepori D, Duvoisin B, Schnyder P, Gudinchet F. Paranasal sinuses in children: size evaluation of maxillary sphenoid and frontal sinuses by magnetic resonance imaging and proposal of volume index percentile curves. Eur Radiol 2002;12(6):1451–8.
[28] Sidler M, Jackowski C, Dirnhofer R, Vock P, Thali M. Use of multi-slice computed tomography in disaster victim identification – advantages and limitations. Forensic Sci Int 2007;169(2–3):118–28.
[29] Štoković N, Trkulja V, Dumić-Čule I, Čuković-Bagić I, Lauc T, Vukičević S, et al. Sphenoid sinus types, dimensions and relationship with surrounding structures. Ann Anat 2016;203:69–76.
[30] Akgul MH, Muluk NB, Burulday V, Kaya A. Is there a relationship between sphenoid sinus types, septation and symmetry; and septal deviation? Eur Arch Otorhinolaryngol 2016;273(12):4321–8.
[31] Guldner C, Pistorius SM, Diogo I, Bien S, Sesterhenn A, Werner JA. Analysis of pneumatization and neurovascular structures of the sphenoid sinus using cone-beam tomography (CBT). Acta Radiol 2012;53(2):214–9.
[32] Hamid O, El Fiky L, Hassan O, Kotb A, El Fiky S. Anatomic variations of the sphenoid sinus and their impact on trans-sphenoid pituitary surgery. Skull Base 2008;18(1):9–15.